Initial Stage of Si(001) Surface Oxidation from First-Principles Calculations

F. Fuchs,* W. G. Schmidt, and F. Bechstedt

Friedrich-Schiller-Universität Jena, 07743 Jena, Germany

Received: January 7, 2005

A comprehensive density-functional theory (DFT) study of the atomic structure, electronic properties, and optical response of the Si(001) surface at the initial stages of oxidation is presented. The most favored adsorption position of a single O atom on top of the (4×2)-reconstructed Si(001) surface is found at the back-bond of the "down" Si dimer atom. There is no energy barrier for oxygen insertion into this bond. The ionization energy of the surface reaches a maximum when the oxidation of the second Si monolayer starts. Oxidation leads to an increase of the energy gap between occupied and empty surface states. The calculated reflectance anisotropy spectroscopy (RAS) data in comparison with experiment suggest a considerable amount of surface disorder already after oxidation of the first monolayer.

1. Introduction

The Si surface oxidation is arguably the most intensively studied subject in surface science, due to its technological relevance for the semiconductor industry and due to the complexity of the surface chemistry.[1] It is because of this complexity that the microscopic details of Si surface oxidation are still not well understood.

Traditional surface characterization techniques, such as scanning tunneling microscopy,[2] photoemission spectroscopy,[3] and electron diffraction techniques,[4] are usually restricted to ultrahigh vacuum conditions and can probe only the uppermost atomic layers. These restrictions do not apply to optical spectroscopies, such as reflectance anisotropy spectroscopy (RAS). Photons penetrate deeply into the substrate and may be used as probes in various environments.[5−8] Indeed, the evolution of the Si(001) surface optical anisotropy during thermal oxidation was monitored, and pronounced changes of the clean surface signal were observed.[9−12] The interpretation of the measured RAS spectra in terms of microscopic surface geometries, however, is difficult.

The geometries of oxidized Si(001) surfaces and Si(001)−SiO_2 interfaces have been probed extensively using ab initio calculations (see, e.g., refs 4 and 13−18). Much less is known, however, about the evolution of the Si(001) surface electronic properties[19] and the change of surface optical response[8,20−22] during oxidation.

The present paper aims at filling this gap. On the basis of accurate total-energy calculations for oxidized Si(001) surface geometries, we relate the structural changes upon oxidation to the surface electronic and optical properties.

2. Method

The calculations are performed within generalized gradient-corrected density-functional theory (DFT-GGA) as implemented in the Vienna Ab Initio Simulation Package (VASP).[23] The electron−ion interaction is described within the projector augmented-wave (PAW) method, allowing for the accurate quantum-mechanical treatment of first-row elements with a relatively small basis set of plane waves. The valence wave functions are expanded into plane waves up to an energy cutoff of 30 Ry.

The Si(001) surface is modeled with a periodically repeated super cell. We use asymmetric, hydrogen-terminated slabs to obtain the structurally relaxed ground state of the various oxidized configurations considered. They contain five relaxed Si atomic layers, including the oxidized ones. To avoid spurious optical asymmetries from the bottom hydrogen layer, the surface optical properties are obtained from symmetric slabs.

Sets corresponding to 64 and 256 k points inside the whole (1×1) surface Brillouin zone (SBZ) are used for reciprocal space integrations to obtain the electronic ground state and the optical spectra, respectively. The reflectance anisotropy of normally incident light for two polarization directions in the surface plane is given by[24]

$$\frac{\Delta r}{r}(\omega) = \frac{8\pi\omega}{c}\mathrm{Im}\left\{\frac{\alpha_{xx}(\omega) - \alpha_{yy}(\omega)}{\epsilon_b(\omega) - 1}\right\} \qquad (1)$$

Here, $\alpha_{ii}(\omega)$ and $\epsilon_b(\omega)$ denote the slab polarizability and bulk dielectric function, respectively, which we calculate in the independent-particle approximation, that is, neglecting excitonic and local-field effects. A scissors operator[25] with an energy shift of 0.5 eV is used to account for the band-gap underestimation in DFT.

3. Results and Discussion

3.1. Structure and Energetics. Clean Si(001) surfaces reconstruct due to the dimerization of the topmost atoms. The dimers are asymmetric, causing a charge transfer from the "down" to the "up" dimer atom. The buckling of the dimer atoms opens a band gap between occupied and unoccupied surface states.[26,27] In the surface ground state, the asymmetric dimers are correlated within the dimer row and between neighboring dimer rows, leading to a $c(4 \times 2)$ reconstruction.[1,28] This $c(4 \times 2)$ reconstruction is the starting point for our calculations.

Although the ground state of the separated reactants, O + Si(001), is a spin-triplet, once the O atom makes a chemical bond with the surface, the singlet potential energy surface (PES)

* Address correspondence to this author. E-mail: fuchs@ifto.unijena.de.

10.1021/jp0501087 CCC: $30.25
Published on Web 08/27/2005

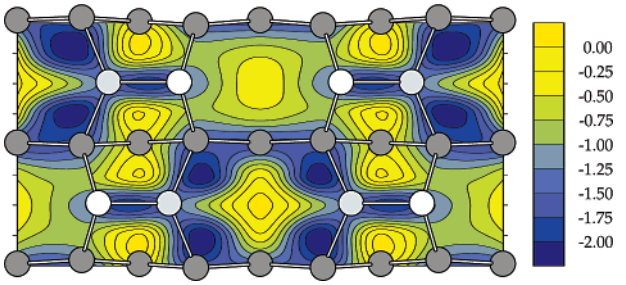

Figure 1. Potential energy surface for the adsorption of one O atom within the $p(4 \times 2)$ surface unit cell. Dark gray (light gray, white) circles indicate the atomic positions of the second- and third-layer (down, up dimer) Si atoms. The energy scale (in eV) refers to the least favored adsorption position.

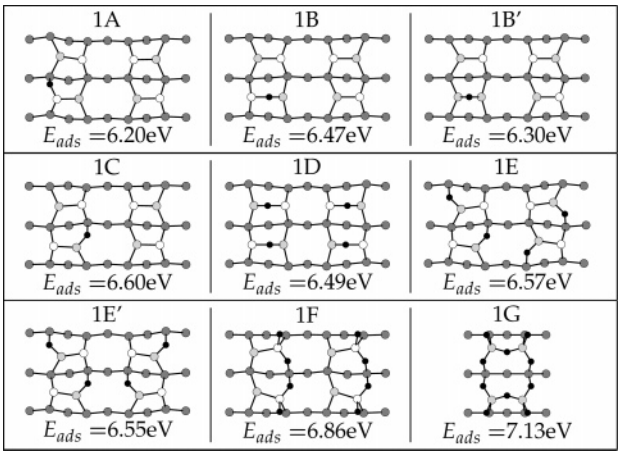

Figure 2. Top view of the models used to describe oxidation of the first Si(001) layer. Black circles represent O atoms; the notation of the Si atoms is the same as that in Figure 1. The calculated adsorption energy (referring to a single spin-triplet O atom) is indicated.

is the ground state.[16] Figure 1 shows the calculated PES for the adsorption of a single oxygen atom within a $p(4 \times 2)$ surface unit cell. The calculations predict local energy minima on top of the Si dimers and global minima at the back-bonds of the down dimer atoms. If allowed to relax fully from the position of the local minimum, the oxygen atom adsorbs about 1.3 Å above the center of the Si dimer. The dimer bond does not break upon adsorption (structure 1B′ in Figure 2). Incorporation of the O atom into the dimer bond (structure 1B in Figure 2) requires it to overcome a small energy barrier and leads to an adsorption energy of 6.47 eV, slightly below the adsorption energy of 6.60 eV released upon back-bond oxidation (1C in Figure 2). The oxidation of the back-bonds of the down dimer atoms is found to be barrierless, in agreement with experiment.[4]

The calculated positions of the global energy minima predicted here agree with previous DFT calculations,[17,19] but not with a recent hybrid quantum-/molecular-mechanics (QM/MM) study,[16] where the effect of dimer buckling was neglected. Indeed, the present calculations show a pronounced influence of the dimer orientation on the adsorption characteristics (cf. Figure 1 as well as structures 1A and 1C in Figure 2).

Further structures considered for the oxidation of the first Si(001) and the uppermost two Si layers are shown in Figures 2 and 3, respectively. The calculated adsorption energies agree within 0.1−0.2 eV with the results by Yamasaki et al.[17] The fact that the values calculated here are consistently slightly lower than the predictions of ref 17 points to a systematic difference, perhaps in the calculation of the isolated O atom.

To investigate the stability of the reacted Si surfaces in dependence on the oxygen chemical potential (μ_O), we calculated the thermodynamic grand-canonical potential per surface unit area[29,30]

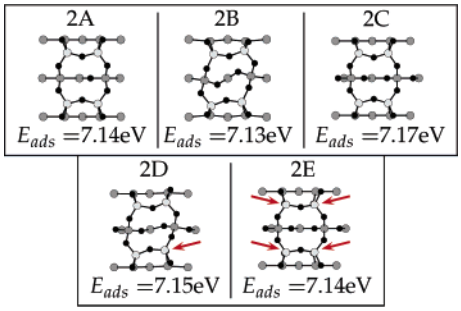

Figure 3. Top view of the models used to describe oxidation of the uppermost two Si(001) layers. Black circles represent O atoms; the notation of the Si atoms is the same as that in Figure 1. The arrows indicate O atoms hidden below Si atoms. The calculated adsorption energy (referring to a single spin-triplet O atom) is indicated.

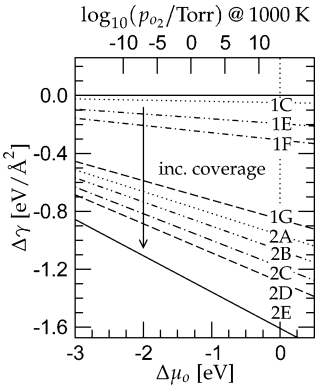

Figure 4. Surface grand-canonical potential versus oxygen chemical potential of some of the structures shown in Figures 2 and 3. The O chemical potential on the bottom *x*-axis is given with respect to molecular oxygen at $T = 0$ K.

$$\Delta\gamma = \frac{1}{A}[E_{\text{oxi}} - E_{\text{clean}} - \mu_O n_O] \qquad (2)$$

where E_{oxi} and E_{clean} are the total energies of the oxidized and clean Si(001) slabs, respectively, and n_O denotes the number of reacted O atoms. For a given temperature, the oxygen chemical potential can be related to an O partial pressure by using the approximation of an ideal two-atomic gas.[31,32] The resulting surface phase diagram for a temperature of 1000 K is shown in Figure 4. It shows that the structure with the highest oxygen coverage studied here, model 2E, is favored over the entire range of the oxygen chemical potential. This indicates that the oxidation proceeds as long as oxygen is available and the reaction barrier can be overcome, in accord with the experimental findings.[1]

3.2. Electronic Properties. To investigate the effect of oxidation on the electronic properties of the Si(001) surface, we calculate the surface bands along the high-symmetry lines Γ−J−K−J′−Γ in the $p(4 \times 2)$ SBZ. The band structure of the configuration 1C is shown in Figure 5. (Figure 2 in ref 33 shows the corresponding figure for the band structure of the clean Si(001) surface, obtained within the same computational method.) Bands belonging to surface states in the oxidized and nonoxidized dimer row are shown by solid and dashed lines, respectively. The largest changes with respect to the band structure of the clean Si(001) surface are observed for states localized in the oxidized dimer row. The two states localized directly at the oxidized dimer are shifted to higher energies along

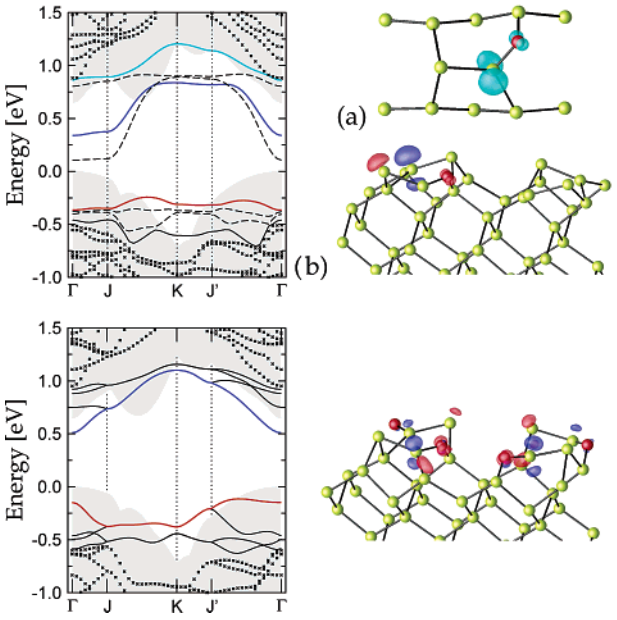

Figure 5. Surface band structures (see text) for the configurations 1C (top) and 1E (bottom). Gray regions indicate the projected Si bulk bands. In the right panels, the orbital characters of the colored surface states at the K point are shown in the respective color. The cyan orbital indicates the unoccupied Si dimer state of the oxidized Si dimer. The isosurface values are 0.1 e/Å^3 (1C) and 0.04 e/Å^3 (1E).

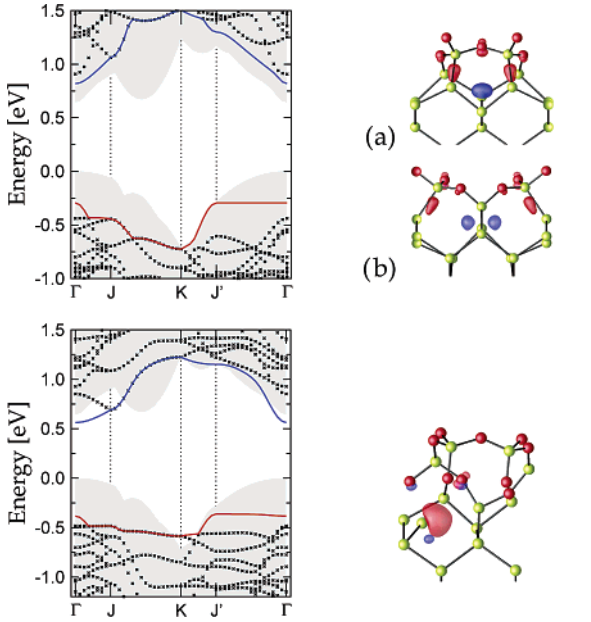

Figure 6. Surface band structures for the configurations 1G (top) and 2E (bottom). Gray regions indicate the projected Si bulk bands. In the right panels, the orbital characters of the uppermost occupied and lowest unoccupied surface states at the K point are shown in red and blue, respectively. The isosurface values are 0.05 e/Å^3 (1G) and 0.08 e/Å^3 (2E).

K−J′. The respective occupied state (red orbital in Figure 5) forms the highest occupied surface state, whereas the respective unoccupied state (indicated in cyan in Figure 5) is almost completely pushed out from the Si bulk band gap region. Both states are not completely derived from silicon orbitals, but show some contributions from oxygen *p* states. The two surface states localized at the nonoxidized dimer of the oxidized row are shifted to lower energies along K−J′ and show a reduced band dispersion along J−K and J′−Γ. The unoccupied state represents the lowest unoccupied surface state at K−J′ (blue orbital in Figure 5).

Structure 1E has a higher oxygen coverage than 1C, but is comparable with respect to the adsorption geometry (cf. Figure 2). In both cases, the back-bonds of the down Si dimer atoms are oxidized. The surface bands of model 1E are shown in Figure 5. For symmetry reasons, all surface bands are degenerate along J−K−J′. Obviously, the oxidation of all four dimer back-bonds leads to a significant increase of the surface band gap. The enhanced band dispersion along Γ−J and K−J′ indicates an increased interaction between electronic states of neighboring dimer rows. Also, the orbital character of the states is changed. In addition to silicon dimer π states and oxygen *p* orbitals, the highest occupied surface state of configuration 1E has contributions from the down dimer atom Si−Si σ back-bond.

If the coverage is increased to one monolayer, that is, configuration 1G, the surface is completely passivated. As shown in Figure 6, all surface state related bands are pushed out of the region of the Si bulk band gap. The highest occupied surface state is localized at the Si dimer back-bonds, with some contribution from the oxygen atoms. Antibonding combinations of Si orbitals in the third atomic layer form the lowest unoccupied surface state.

Further increase of the oxygen coverage may lead to the reappearance of surface states at the Si bulk band edges. This is shown for the case of the 2E model in the lower part of Figure 6. At the K point of the SBZ, the highest occupied surface state separates energetically from the continuum of bulk states. It results from the nonbonding electrons becoming available by the adsorption of a bridging oxygen between Si atoms of the second layer, leaving a third layer Si atom 2-fold coordinated.[17] The respective orbital shows a sp^2-like character. It is localized near the 2-fold bound Si atom right at the interface between the oxidized layers and bulk Si. Unoccupied bound surface states can be found around the Γ, J, and K points of the SBZ. As shown in Figure 6, they are interface-localized, as well.

The ionization energy is defined as the energy difference between the vacuum level and the valence-band maximum. Its variation upon adsorption is related to the formation of a macroscopic surface dipole and is given by the difference of the respective effective electron potentials

$$V(\boldsymbol{r}) = V_{\mathrm{ps}}^{\mathrm{loc}}(\boldsymbol{r}) + V_{\mathrm{H}}(\boldsymbol{r}) + V_{\mathrm{xc}}(\boldsymbol{r}) \qquad (3)$$

for the clean and adsorbed surfaces in the bulk region of the slab.[34] Here, $V_{\mathrm{ps}}^{\mathrm{loc}}(\boldsymbol{r})$, $V_{\mathrm{H}}(\boldsymbol{r})$, and $V_{\mathrm{xc}}(\boldsymbol{r})$ denote the local part of the pseudopotential, the Hartree potential, and the exchange-correlation potential in GGA, respectively. The difference of the ionization energy with respect to the clean $c(4 \times 2)$-reconstructed surface in dependence of the oxygen coverage is shown in Figure 7. Since oxygen is significantly more electronegative than silicon, one expects an electron transfer from the substrate to the adsorbate, leading to a surface dipole layer that should increase the ionization energy.[35] Indeed, the calculations predict, depending on the coverage, an increase in the ionization energy by up to 1 eV. Interestingly, initially, the ionization energy increases until a coverage of 2.5 oxygen atoms per (1×1) surface unit cell is reached. For higher coverages, the ionization energy decreases, again, but remains higher than that of the clean Si(001) surface. Obviously, there is a large scatter in the predicted changes of the ionization energy, depending on the structural model and coverage. It is difficult to compare the results of our microscopic calculations with measurement because little is known about the actual structure of the oxidized surface. In dependence on exposure time, oxygen partial

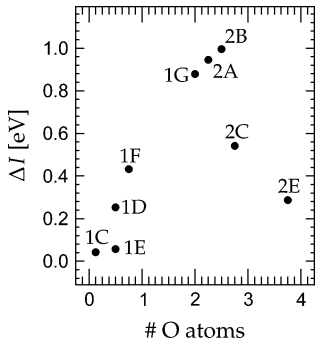

Figure 7. Calculated change of ionization energy upon oxidation versus the number of oxygen atoms adsorbed inside the $p(1 \times 1)$ surface unit cell.

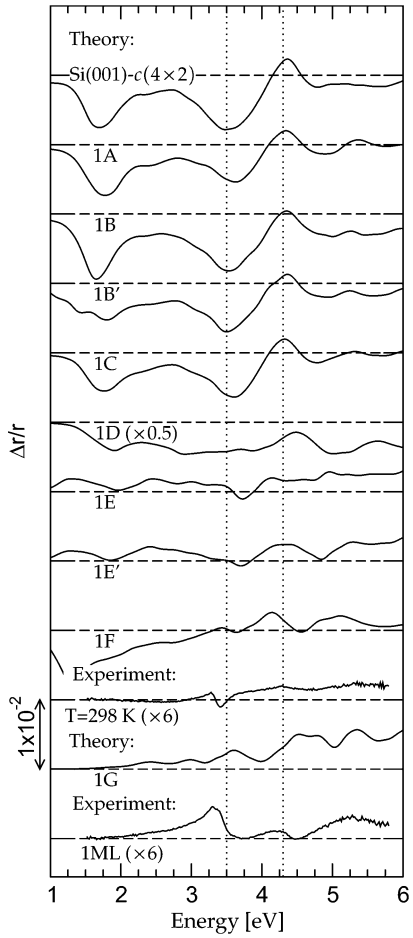

Figure 8. RAS spectra $Re\{(r_{[\bar{1}10]} - r_{[1\bar{1}0]})/\langle r\rangle\}$ calculated for the oxidized configurations shown in Figure 2 are compared with measured data from ref 12. Dotted lines indicate the E_1 and E_2 critical-point energies.

pressure, and temperature, values of ΔI between 0 and 0.35 eV are reported.[36,37]

3.3. Optical Response. RAS spectra calculated for the clean $c(4 \times 2)$ Si(001) surface and the oxidation models 1A−1G are compared with experimental data from ref 12 in Figure 8. The optical anisotropy of the clean surface shows a strong dimer state related minimum at 1.7 eV. In addition, there are pronounced features for photon energies slightly below/above the E_1/E_2 bulk critical point energies of silicon at 3.5/4.3 eV resulting from surface-perturbed bulk states. The calculated spectrum agrees with data measured on highly oriented, single-domain Si(001) surfaces.[12,38] For vicinal Si(001) surfaces, an additional step-related feature at about 3 eV is found.[39,40]

The calculated spectra 1A−1C show the modification of the surface optical anisotropy in the very first stages of oxidation. The general line shape of the clean surface spectrum is preserved, but the Si dimer state related feature is modified slightly with respect to its energy position and magnitude. The feature is reduced with respect to the clean surface when oxygen attacks a dimer back-bond (1A or 1C) or is adsorbed above the Si dimer (1B′). In contrast, an enhancement of this low-energy structure occurs if the oxygen atom bridges the Si dimer atoms (1B). The same trend is found for the E_1 feature, while the magnitude of the E_2 feature is reduced in any case.

For increased coverage, the RAS signal changes drastically, as shown by the spectra for the models 1D−1G in Figure 8. The dimer state related feature at 1.7 eV is strongly reduced in magnitude. This is to be expected because the corresponding electronic states are pushed out of the band gap region, as discussed above. However, also, the optical anisotropies close to the bulk critical points are modified. If one compares structures with similar adsorption motifs, but different coverages, such as the Si dimer oxidation in models 1B and 1D, for example, one notices that the corresponding RAS spectra are not related to each other by a simple scaling relation. This is due to the strong dimer−dimer interaction that shows up in the optical response of the Si(001) surface.[40,41]

The E_1 feature of the calculated spectrum 1F remotely resembles the experimental data measured after room-temperature oxidation of Si(001) (cf. Figure 8). However, the observed vanishing of the anisotropy signal for photon energies below 2.5 eV is not reproduced. The RAS signal calculated for configuration 1G is positive throughout the energy range probed. This is unique among the structures investigated and agrees with the experimental findings after 8 s oxidation at 1000 K that were assigned to an oxide thickness of 1 monolayer by Yasuda et al.[12] The quenching of the RAS signal below 2.5 eV is another feature common to both experiment and calculation for 1G. This results from the complete removal of surfaces states from the fundamental gap (cf. Figure 6).

There is, thus, some agreement between experiment and theory. However, the overall unsatisfactory description of the line shape measured after oxidation of one monolayer indicates that the actual surface resulting from the oxidation of the uppermost Si layer is not described by a well-ordered structure corresponding to one of the models investigated here. The signal is likely to be affected by a considerable amount of disorder. This explanation is in agreement with high-energy electron diffraction data[4] and scanning tunneling microscopy images of Si(001) surfaces exposed to oxygen.[2] In fact, for coverages higher than one monolayer, we have recently shown that the measured RAS signal can be explained by assuming an optically isotropic overlayer, that is, a mesoscopically disordered silicon dioxide film on top of bulk silicon strained by the insertion of oxygen atoms.[22] Most relevant for comparison with experiment are, thus, the spectra calculated for submonolayer coverage. Unfortunately, at present, there are no RAS experiments available that address the initial adsorption configurations.

4. Summary

In summary, we studied the atomic structures and the related electronic and optical properties of the oxidized Si(001) surface by means of *first-principles* calculations. A highly structured potential energy surface was found, with global minima at the back-bonds of the down Si dimer atoms. Oxygen incorporation into these Si bonds was found to be barrierless. For the structures probed in this study, the ionization energy increased with respect

to the clean Si(001) surface. The calculated surface band structures show a widening of the band gap between occupied and empty surface states for increasing oxygen coverage. However, even for thick oxide overlayers, there may be bound interface states close to the Si bulk band gap edges. The surface optical anisotropy is found to be sensitive to the structural details of the adsorption configuration. Comparison with the experimental data suggests, however, that an appreciable amount of disorder is present at the surface already after oxidation of the first Si monolayer.

Acknowledgment. Grants of computer time from the Leibniz-Rechenzentrum München and the Höchstleistungsrechenzentrum Stuttgart are gratefully acknowledged. The work was financially supported by the EU Network of Excellence NANOQUANTA (Contract No. NMP4-CT-2004-500198).

References and Notes

(1) Dabrowski, J.; Müssig, H.-J. *Silicon Surfaces and Formation of Interfaces*; World Scientific: Singapore, 2000.
(2) Fujita, K.; Watanabe, H.; Ichikawa, M. *Appl. Phys. Lett.* **1997**, *70*, 2807.
(3) Harada, Y.; Niwa, M.; Nagatomi, T.; Shimizu, R. *Jpn. J. Appl. Phys.* **2000**, *39*, 560.
(4) Watanabe, H.; Kato, K.; Uda, T.; Fujita, K.; Ichikawa, M.; Kawamura, T.; Terakura, K. *Phys. Rev. Lett.* **1998**, *80*, 345.
(5) Kamiya, I.; Aspnes, D. E.; Tanaka, H.; Florez, L. T.; Harbison, J. P.; Bhat, R. *Phys. Rev. Lett.* **1992**, *68*, 627.
(6) Aspnes, D. E. *Solid State Commun.* **1997**, *101*, 85.
(7) Richter, W. *Philos. Trans. R. Soc. London, Ser. A* **1993**, *344*, 453.
(8) Schmidt, W. G.; Fuchs, F.; Hermann, A.; Seino, K.; Bechstedt, F.; Passmann, R.; Wahl, M.; Gensch, M.; Hinrichs, K.; Esser, N.; Wang, S.; Lu, W.; Bernholc, J. *J. Phys.: Condens. Matter* **2004**, *16*, S4323.
(9) Yasuda, T.; Nishizawa, M.; Kumagai, N.; Yamasaki, S.; Oheda, H.; Yamabe, K. *Thin Solid Films* **2004**, *455*−*456*, 759.
(10) Yasuda, T.; Kumagai, N.; Nishizawa, M.; Yamasaki, S.; Oheda, H.; Yamabe, K. *Phys. Rev. B* **2003**, *67*, 195338.
(11) Matsudo, T.; Ohta, T.; Yasuda, T.; Nishizawa, M.; Miyata, N.; Yamasaki, S.; Shklyaev, A. A.; Ichikawa, M. *J. Appl. Phys.* **2002**, *91*, 3637.
(12) Yasuda, T.; Yamasaki, S.; Nishizawa, M.; Miyata, N.; Shklyaev, A.; Ichikawa, M.; Matsudo, T.; Ohta, T. *Phys. Rev. Lett.* **2001**, *87*, 037403.
(13) Kageshima, H.; Shiraishi, K. *Phys. Rev. Lett.* **1998**, *81*, 5936.
(14) Kato, K.; Uda, T.; Terakura, K. *Phys. Rev. Lett.* **1998**, *80*, 2000.
(15) Kato, K.; Uda, T. *Phys. Rev. B* **2000**, *62*, 15978.
(16) Choi, C. H.; Liu, D.-J.; Evans, J. W.; Gordon, M. S. *J. Am. Chem. Soc.* **2002**, *124*, 8730.
(17) Yamasaki, T.; Kato, K.; Uda, T. *Phys. Rev. Lett.* **2003**, *91*, 146102.
(18) Bongiorno, A.; Pasquarello, A. *Phys. Rev. Lett.* **2004**, *93*, 086102.
(19) Uchiyama, T.; Tsukada, M. *Phys. Rev. B* **1996**, *53*, 7917.
(20) Nakayama, T.; Murayama, M. *Appl. Phys. Lett.* **2000**, *77*, 4286.
(21) Incze, A.; Del Sole, R.; Onida, G. *Phys. Rev. B* **2005**, *71*, 035350.
(22) Fuchs, F.; Schmidt, W. G.; Bechstedt, F. *Phys. Rev. B*, in press.
(23) Kresse, G.; Furthmüller, J. *Comput. Mater. Sci.* **1996**, *6*, 15.
(24) Del Sole, R. *Solid State Commun.* **1981**, *37*, 537.
(25) Del Sole, R.; Girlanda, R. *Phys. Rev. B* **1993**, *48*, 11789.
(26) Ramstad, A.; Brocks, G.; Kelly, P. J. *Phys. Rev. B* **1995**, *51*, 14504.
(27) Krüger, P.; Pollmann, J. *Phys. Rev. Lett.* **1995**, *74*, 1155.
(28) Seino, K.; Schmidt, W. G.; Bechstedt, F. *Phys. Rev. Lett.* **2004**, *93*, 036101.
(29) Qian, G.-X.; Martin, R. M.; Chadi, D. J. *Phys. Rev. B* **1988**, *38*, 7649.
(30) Bechstedt, F. *Principles of Surface Physics*; Springer-Verlag: Berlin, 2003.
(31) Van de Walle, C. G.; Neugebauer, J. *Phys. Rev. Lett.* **2002**, *88*, 066103.
(32) Hahn, P. H.; Schmidt, W. G. *Surf. Rev. Lett.* **2003**, *10*, 163.
(33) Preuss, M.; Schmidt, W. G.; Bechstedt, F. *J. Phys. Chem. B* **2004**, *108*, 7809.
(34) Schmidt, W. G.; Bechstedt, F.; Srivastava, G. P. *Surf. Sci. Rep.* **1996**, *25*, 141.
(35) Mönch, W. *Semiconductor Surfaces and Interfaces*, 3rd ed.; Series in Surface Sciences; Springer: Berlin, Heidelberg, New York, 2001; Vol. 26.
(36) Law, J. T. *J. Appl. Phys.* **1961**, *32*, 600.
(37) Ranke, W.; Xing, Y. R. *Phys. Rev. B* **1985**, *31*, 2246.
(38) Shioda, R.; van der Weide, J. *Phys. Rev. B* **1998**, *57*, R6823.
(39) Kipp, L.; Biegelsen, D. K.; Northrup, J. E.; Swartz, L.-E.; Bringans, R. D. *Phys. Rev. Lett.* **1996**, *76*, 2810.
(40) Schmidt, W. G.; Bechstedt, F.; Bernholc, J. *Phys. Rev. B* **2001**, *63*, 045322.
(41) Kress, C.; Shkrebtii, A. I.; Del Sole, R. *Surf. Sci.* **1997**, *377*, 398.